Highly Stable Electrochromic Polyamides Based on *N,N*-Bis(4-aminophenyl)-*N′,N′*-bis(4-*tert*-butylphenyl)-1,4-phenylenediamine

SHENG-HUEI HSIAO,[1] GUEY-SHENG LIOU,[2] HUI-MIN WANG[1]

[1]Department of Chemical Engineering and Biotechnology, National Taipei University of Technology, 1 Chunghsiao East Road, Section 3, Taipei 10608, Taiwan

[2]Institute of Polymer Science and Engineering, National Taiwan University, 1 Roosevelt Road, Section 4, Taipei 10617, Taiwan

Received 25 December 2008; accepted 25 January 2009
DOI: 10.1002/pola.23323
Published online in Wiley InterScience (www.interscience.wiley.com).

ABSTRACT: A new triphenylamine-containing aromatic diamine monomer, *N,N*-bis (4-aminophenyl)-*N′,N′*-bis(4-*tert*-butylphenyl)-1,4-phenylenediamine, was synthesized by an established synthetic procedure from readily available reagents. A novel family of electroactive polyamides with di-*tert*-butyl-substituted *N,N,N′,N′*-tetraphenyl-1,4-phenylenediamine units were prepared via the phosphorylation polyamidation reactions of the newly synthesized diamine monomer with various aromatic or aliphatic dicarboxylic acids. All the polymers were amorphous with good solubility in many organic solvents, such as *N*-methyl-2-pyrrolidinone (NMP) and *N,N*-dimethylacetamide, and could be solution-cast into tough and flexible polymer films. The polyamides derived from aromatic dicarboxylic acids had useful levels of thermal stability, with glass-transition temperatures of 269–296 °C, 10% weight-loss temperatures in excess of 544 °C, and char yields at 800 °C in nitrogen higher than 62%. The dilute solutions of these polyamides in NMP exhibited strong absorption bands centered at 316–342 nm and photoluminescence maxima around 362–465 nm in the violet-blue region. The polyamides derived from aliphatic dicarboxylic acids were optically transparent in the visible region and fluoresced with a higher quantum yield compared with those derived from aromatic dicarboxylic acids. The hole-transporting and electrochromic properties were examined by electrochemical and spectro-electrochemical methods. Cyclic voltammograms of the polyamide films cast onto an indium-tin oxide-coated glass substrate exhibited two reversible oxidation redox couples at 0.57–0.60 V and 0.95–0.98 V versus Ag/AgCl in acetonitrile solution. The polyamide films revealed excellent elcterochemical and electrochromic stability, with a color change from a colorless or pale yellowish neutral form to green and blue oxidized forms at applied potentials ranging from 0.0 to 1.2 V. These anodically coloring polymeric materials showed interesting electrochromic properties, such as high coloration efficiency (CE = 216 cm^2/C for the green coloring) and high contrast ratio of optical transmittance change ($\Delta T\%$) up to 64% at 424 nm and 59% at 983 nm for the green coloration, and 90% at 778 nm for the blue coloration. The electroactivity of the polymer remains intact even after cycling 500 times between its

Additional Supporting Information may be found in the online version of this article.

Correspondence to: S.-H. Hsiao (E-mail: shhsiao@ntut.edu.tw)

Journal of Polymer Science: Part A: Polymer Chemistry, Vol. 47, 2330–2343 (2009)

neutral and fully oxidized states. © 2009 Wiley Periodicals, Inc. J Polym Sci Part A: Polym Chem 47: 2330–2343, 2009

Keywords: electroactivity; electrochemistry; electrochromism; *N,N,N′,N′*-tetraphenyl-1,4-phenylenediamine; polyamides; triphenylamine

INTRODUCTION

An electrochromic material is one where a reversible color change takes place upon reduction (gain of electrons) or oxidation (loss of electrons), on passage of electrical current after the application of an appropriate electrode potential.[1,2] Electrochromic materials, both organic and inorganic, have promising applications in light-attenuation, displays, and analysis.[3] Electrochromic applications based on π-conjugated polymers have received increased attention owing to their ease of color-tuning, fast switching times, and high contrast ratios.[4–6] Among the available electrochromic polymers, poly(3,4-ethylenedioxythiophene) and its derivatives have been extensively studied because of the merit of their high stability, which arises from the electron-donating ethylenedioxy group.[5–9]

Triarylamine derivatives are well known for photo and electroactive properties that find optoelectronic applications as photoconductors, hole-transporters, and light-emitters.[10,11] Triarylamines can be easily oxidized to form stable radical cations, and the oxidation process is always associated with a noticeable change of coloration. Thus, many triarylamine-based electrochromic polymers have been reported in literature.[12–15] In recent years, we have developed a number of high-performance polymers (e.g., aromatic polyamides and polyimides) carrying the triphenylamine (TPA) unit as an electrochromic functional moiety.[16–22] Our strategy was to synthesize the TPA-containing monomers such as diamines and dicarboxylic acids that were then reacted with the corresponding comonomers through conventional polycondensation techniques. The obtained polymers possessed characteristically high molecular weights and high thermal stability. Because of the incorporation of packing-disruptive, propeller-shaped TPA units along the polymer backbone, most of these polymers exhibited good solubility in polar organic solvents. They may form uniform, transparent amorphous thin films by solution casting and spin-coating methods. This is advantageous for their ready fabrication of large-area, thin-film devices.

The anodic oxidation pathways of TPA derivatives were well studied.[23] The electrogenerated cation radical of TPA is not stable and could dimerize to form tetraphenylbenzidine by tail to tail coupling with loss of two protons per dimer. When the phenyl groups were incorporated by electron-donating substituents such as *tert*-butyl and methoxy groups at the *para*-position of TPA, the coupling reactions were greatly prevented by affording stable cationic radicals and lowering the oxidation potentials.[24–26] The redox property, electron-transfer process, and multicoloring electrochromic behavior of the polymers bearing *N,N,N′,N′*-tetraphenyl-1,4-phenylenediamine (TPPA) segments are interesting for opto-electronic applications.[27–29] In this article, we therefore synthesized the new diamine, *N,N*-bis(4-aminophenyl)-*N′,N′*-bis(4-*tert*-butylphenyl)-1,4-phenylenediamine (**4**), and its derived polyamides containing the electroactive TPPA segment. With such a configuration, the electrochemically active sites of the pendent phenyl groups are blocked, giving the polyamides extra redox stability. As a result, the resultant polyamides are expected to exhibit an enhanced electrochemical and electrochromic stability, which is of great importance in practical applications.

EXPERIMENTAL

Materials

Dimethyl sulfoxide (DMSO), pyridine and *N*-methyl-2-pyrrolidone (NMP) were dried over calcium hydride for 24 h, distilled under reduced pressure, and stored over 4 Å molecular sieves in a sealed bottle. The commercially available aromatic and aliphatic dicarboxylic acids that included terephthalic acid (**5a**) (Wako), isophthalic acid (**5b**) (Wako), 4,4′-biphenydicarboxylic acid (**5c**) (TCI), 4,4′-dicarboxydiphenyl ether (**5d**) (TCI), bis(4-carboxyphenyl) sulfone (**5e**) (New Japan Chemicals Co.), 2,2-bis(4-carboxyphenyl) hexafluoropropane (**5f**) (TCI), 1,4-naphthalenedicarboxylic acid (**5g**) (Wako), 2,6-naphthalenedicarboxylic acid (**5h**) (TCI), 1,4-cyclohexanedicarboxylic acid (**5i**) (TCI), adipic acid (**5j**) (Acros) were used as-received. Calcium chloride was dried under vacuum at 150 °C for 6 h before use.

Tetrabutylammonium perchlorate (TBAP) (ACROS) were recrystallized twice by ethyl acetate under nitrogen atmosphere and then dried *in vacuo* before use. All other reagents were used as-received from commercial sources.

Monomer Synthesis

4,4′-Di-tert-butyl-4″-nitrotriphenylamine (1)

A mixture of 4.0 g (0.1 mol) of sodium hydride (NaH) (60% in mineral oil) and 28.1 g (0.1 mol) of bis(4-*tert*-butylphenyl)amine in 150 mL of anhydrous DMSO was stirred at room temperature for about 30 min. Then, 14.1 g (0.1 mol) of *p*-fluoronitrobenzene were added to the suspension solution, and the mixture was heated with stirring at 140 °C for 18 h. After cooling to room temperature, the reaction solution was poured into 1.5 L of stirred methanol/water (3:1), and the olivine precipitate was collected by filtration and washed thoroughly with methanol and water. Recrystallization from DMSO/MeOH yielded 26.6 g (66% in yield) of the desired nitro compound (**1**) as yellow crystals with a mp of 178–179 °C.

IR (KBr): 2958 cm^{-1} (*t*-butyl C—H str), 1321, 1585 cm^{-1} (—NO_2 str). ^1H NMR (500 MHz, DMSO-d_6, δ, ppm): 1.29 (s, 18H, *t*-butyl), 6.73 (d, $J = 9.3$ Hz, 2H, H_c), 7.19 (d, $J = 8.5$ Hz, 4H, H_b), 7.47 (d, $J = 8.5$ Hz, 4H, H_a), 8.05 (d, $J = 9.3$ Hz, 2H, H_d). ^{13}C NMR (125 Hz, δ, ppm, DMSO-d_6): 31.00 (C^1), 34.22 (C^2), 115.80 (C^8), 125.61 (C^9), 126.43 (C^5), 126.89 (C^4), 138.40 (C^{10}), 142.14 (C^3), 148.68 (C^6), 153.42 (C^7). The IR, ^1H NMR, and ^{13}C NMR spectra of compound **1** are illustrated in Supporting Information Figures S1 and S2.

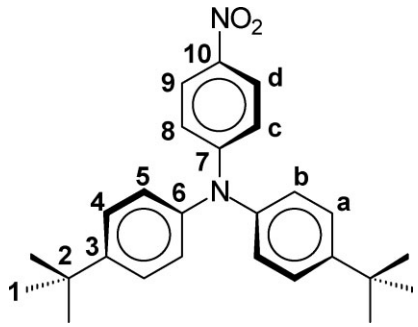

4-Amino-4′,4″-di-tert-butyltriphenylamine (2)

In a 500 mL round-bottom flask, 10 g (0.025 mol) of nitro compound **1**, 0.2 g of 10 wt % Pd/C, 5 mL hydrazine monohydrate and 150 mL of ethanol was heated in nitrogen flow at a reflux temperature for 12 h. The solution was filtered to remove the catalyst, and the filtrate was distilled to remove the solvent. Recrystallization from hexane to give 7.4 g (80% in yield) of white crystals with a mp of 139–141 °C.

IR (KBr): 3444, 3363 cm^{-1} (—NH_2 str), 2960 cm^{-1} (*t*-butyl C—H str). ^1H NMR (500 MHz, DMSO-d_6, δ, ppm): 1.24 (s, 18H, *t*-butyl), 5.00 (s, 2H, —NH_2), 6.55 (d, $J = 8.6$ Hz, 2H, H_c), 6.77 (d, $J = 8.6$ Hz, 2H, H_d), 6.81 (d, $J = 8.7$ Hz, 4H, H_b), 7.19 (d, $J = 8.7$ Hz, 4H, H_a). ^{13}C NMR (125 Hz, δ, ppm, DMSO-d_6): 31.21 (C^1), 33.70 (C^2), 114.85 (C^9), 120.90 (C^5), 125.57 (C^4), 127.72 (C^8), 135.54 (C^7), 142.96 (C^3), 145.49 (C^6), 145.78 (C^{10}). The IR, ^1H NMR, and ^{13}C NMR spectra of compound **2** are illustrated in Supporting Information Figures S1 and S3.

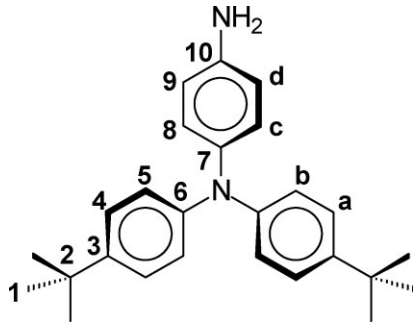

N,N-Bis(4-tert-butylphenyl)-N′,N′-bis (4-nitrophenyl)-1,4-phenylenediamine (3)

In a 250 mL round-bottom flask equipped with a stirring bar, a mixture of 7.45 g (0.02 mol) of 4-amino-4′,4″-di-*tert*-butyltriphenylamine (**2**), 5.7 g (0.04 mol) of *p*-fluoronitrobenzene, and 6.1 g of cesium fluoride (CsF) in 80 mL of DMSO was heated at 150 °C for about 18 h. After cooling, the mixture was poured into 800 mL mixed solution of methanol/water (4:1), and the precipitate was collected by filtration and washed thoroughly with methanol and water. Recrystallization from DMF/methanol yielded 7.8 g (64% in yield) of the desired dinitro compound **3** as red crystals with a mp of 249–251 °C.

IR (KBr): 2960 cm^{-1} (*t*-butyl C—H stretch), 1321, 1585 cm^{-1} (—NO_2 stretch). ^1H NMR (500 MHz, DMSO-d_6, δ, ppm) (see Supporting Information Figure S4): 1.29 (s, 18H, *t*-butyl), 6.96 (d, $J = 8.8$ Hz, 2H, H_c), 7.04 (d, $J = 8.6$ Hz, 4H, H_b), 7.12 (d, $J = 8.8$ Hz, 2H, H_d), 7.23 (d, $J = 9.2$ Hz, 4H, H_e), 7.37 (d, $J = 8.6$ Hz, 4H, H_a), 8.19 (d, $J = 9.1$ Hz, 4H, H_f).

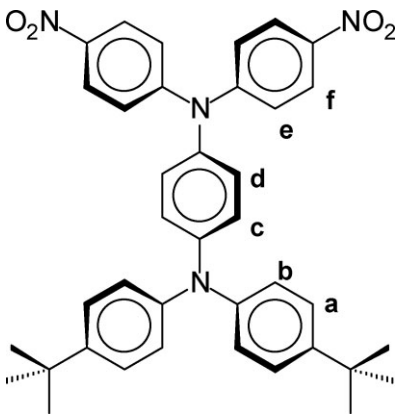

N,N-Bis(4-aminophenyl)-N′,N′-bis(4-tert-butylphenyl)-1,4-phenylenediamine (4)

In a 500 mL round-bottom flask, 7.6 g (0.012 mol) of dinitro compound (**3**), 0.1 g of 10 wt % Pd/C, 5 mL hydrazine monohydrate and 100 mL of ethanol was heated in nitrogen flow at a reflux temperature for 12 h. The solution was filtered hot to remove Pd/C and the filtrate was added water. Recrystallization from toluene yielded 4.5 g (64% yield) of the desired diamine monomer **4** as pink crystals with a mp of 211–213 °C.

IR (KBr): 3444, 3359 cm^{-1} (—NH_2 stretch), 2960 cm^{-1} (*t*-butyl C—H stretch). ANAL. Calcd for $C_{38}H_{42}N_4$ (554.77): C, 82.27 %; H, 7.63 %; N, 10.10 %. Found: C, 82.22 %; H, 7.46 %; N, 10.07 %. ^{1}H NMR (500 MHz, DMSO-d_6, δ, ppm): 1.24 (s, 18H, *t*-butyl), 4.92 (s, 4H, —NH_2), 6.53 (d, $J = 8.6$ Hz, 4H, H_f), 6.59 (d, $J = 8.9$ Hz, 2H, H_d), 6.78 (d, $J = 8.9$ Hz, 2H, H_c), 6.81 (d, $J = 8.6$ Hz, 4H, H_e), 6.83 (d, $J = 8.7$ Hz, 4H, H_b), 7.22 (d, $J = 8.7$ Hz, 4H, H_a). ^{13}C NMR (125 Hz, δ, ppm, DMSO-d_6): 31.14 (C^1), 33.74 (C^2), 114.73 (C^{13}), 117.92 (C^9), 121.49 (C^5), 125.72 (C^4), 126.44 (C^8), 126.93 (C^{12}), 136.08 (C^{11}), 137.60 (C^7), 143.47 (C^3), 145.18 (C^{14}), 145.25 (C^6), 145.95 (C^{10}).

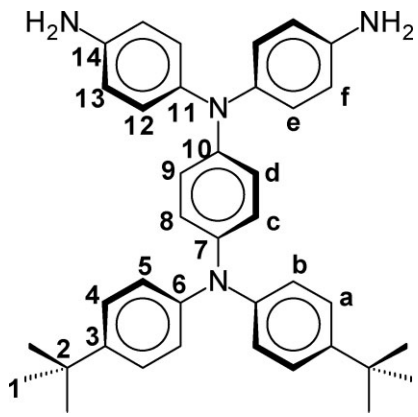

Polymer Synthesis

The synthesis of polyamide **6a** is used as an example to illustrate the general synthetic route. A mixture of 0.555 g (1.00 mmol) of the diamine monomer **4**, 0.166 g (1.00 mmol) of terephthalic acid (**5a**), 0.15 g of calcium chloride, 1.00 mL of triphenyl phosphite (TPP), 0.25 mL of pyridine, and 1.00 mL of NMP was heated with stirring at 120 °C for 3 h. The highly viscous polymer solution was poured slowly into 200 mL of stirring methanol giving rise to a stringy, fiber-like precipitate that was collected by filtration, washed thoroughly with hot water and methanol, and dried under vacuum at 100 °C. Reprecipitations from *N*,*N*-dimethylacetamide (DMAc) into methanol were carried out twice for further purification. The inherent viscosity of the obtained polyamide **6a** was 0.71 dL/g, measured at a concentration of 0.5 g/dL in DMAc-5 wt % LiCl at 30 °C. The IR spectrum of **6a** (film) exhibited characteristic amide absorption bands at 3300 cm^{-1} (N—H str), 2960 cm^{-1} (*t*-butyl C—H str), and 1653 cm^{-1} (amide carbonyl).

Preparation of the Polyamide Films

A solution of the polymer was made by dissolving about 0.7 g of the polyamide sample in 10 mL of DMAc. The homogeneous solution was poured into an 11-cm glass Petri dish, which was placed in a 90 °C oven for 3 h to remove most of the solvent; then the semidried film was further dried *in vacuo* at 170 °C for 7 h. The obtained films were about 40–60 μm thick and were used for X-ray diffraction measurements, solubility tests, and thermal analyses.

Measurements

Infrared (IR) spectra were recorded on a Horiba FT-720 FTIR spectrometer. Elemental analyses were run in a Heraeus VarioEL III CHNS elemental analyzer. ^{1}H and ^{13}C NMR spectra were measured on a Bruker AVANCE 500 FT-NMR system with tetramethylsilane as an internal standard. The inherent viscosities were determined with a Cannon-Fenske viscometer at 30 °C. Wide-angle X-ray diffraction (WAXD) measurements were performed at room temperature (~25 °C) on a Shimadzu XRD-6000 X-ray diffractometer with a graphite monochromator (operating at 40 kV and 30 mA), using nickel-filtered Cu-Kα radiation (λ = 1.5418 Å). The scanning rate was 2 °C/min over a range of $2\theta = 10\sim40°$. Thermogravimetric

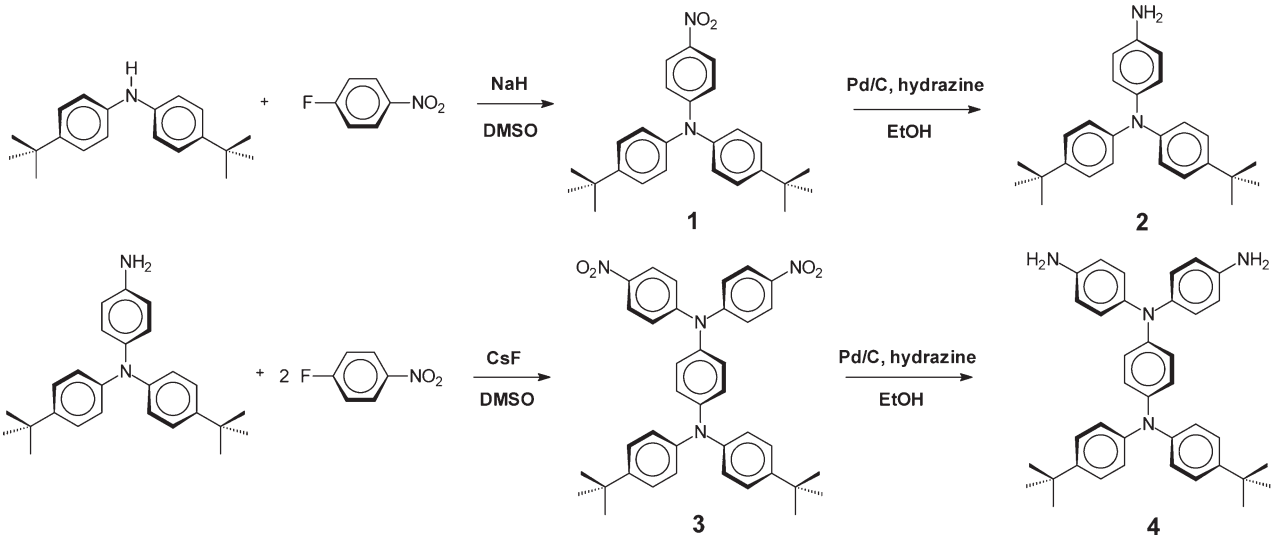

Scheme 1. Synthetic route to the diamine monomer **4**.

analysis (TGA) was performed with a Perkin-Elmer Pyris 1 TGA. Experiments were carried out on ~4–6 mg of samples heated in flowing nitrogen or air (flow rate = 40 cm^3/min) at a heating rate of 20 °C/min. DSC analyses were performed on a Perkin-Elmer Pyris 1 DSC at a scan rate of 20 °C/min in flowing nitrogen. Thermomechanical analysis (TMA) was determined with a Perkin–Elmer TMA 7 instrument. The TMA experiments were carried out from 50 to 400 °C at a scan rate of 10 °C/min with a penetration probe 1.0 mm in diameter under an applied constant load of 10 mN. Softening temperatures (T_s) were taken as the onset temperatures of probe displacement on the TMA traces. Ultraviolet-visible (UV–Vis) spectra of the polymer films were recorded on an Agilent 8453 UV–Visible spectrometer. Electrochemistry was performed with a CHI 611C electrochemical analyzer. Voltammograms are presented with the positive potential pointing to the left and with increasing anodic currents pointing downwards. Cyclic voltammetry (CV) was conducted with the use of a three-electrode cell in which indium-tin oxide (ITO; polymer films area about 0.8 cm × 1.25 cm) was used as a working electrode. A platinum wire was used as an auxiliary electrode. All cell potentials were taken with the use of a home-made Ag/AgCl, KCl (sat.) reference electrode. Ferrocene was used as an external reference for calibration (+0.48 V vs. Ag/AgCl). Spectro-electrochemistry analyses were carried out with an electrolytic cell, which was composed of a 1 cm cuvette, ITO as a working electrode, a platinum wire as an auxiliary electrode, and an Ag/AgCl reference electrode. Absorption spectra in the spectroelectrochemical experiments were also measured with an Agilent 8453 UV–Visible spectrophotometer. Coloration efficiency (CE) is derived from the equation: $\eta = \Delta OD/Q$, ΔOD is optical density change at specific absorption wavelength and Q is ejected charge determined from the *in situ* experiments. Photoluminescence (PL) spectra were measured with a Varian Cary Eclipse fluorescence spectrophotometer. Fluorescence quantum yields (Φ_F) values of the samples in NMP were measured by using quinine sulfate in 1*N* H_2SO_4 as a reference standard ($\Phi_F = 54.6\%$).[30] All corrected fluorescence excitation spectra were found to be equivalent to their respective absorption spectra.

RESULTS AND DISCUSSION

Monomer Synthesis

The new diamine monomer, *N,N*-bis(4-aminophenyl)-*N′,N′*-bis(4-*tert*-butylphenyl)-1,4-phenylenediamine (**4**), was synthesized by a four-step reaction sequence starting from bis(4-*tert*-butylphenyl)amine and *p*-fluoronitrobenzene, as outlined in Scheme 1. In the first step, the intermediate compound, 4,4′-di-*tert*-butyl-4″-nitrotriphenylamine (**1**) was synthesized by nucleophilic aromatic fluoro-displacement reaction of *p*-fluoronitrobenzene with the amide ion of bis(4-*tert*-butylphenyl)amine formed *in situ* by sodium hydride. Reduction of the nitro group of compound **1** by means of hydrazine and Pd/C gave 4-

amino-4′,4″-di-*tert*-butyltriphenylamine (**2**). The target diamine monomer **4** was prepared by hydrazine Pd/C-catalyzed reduction of dinitro compound **3** resulting from the cesium fluoride (CsF)-assisted *N,N*-diarylation reaction of compound **2** with two equivalent amount of *p*-fluoronitrobenzene. IR, ^{1}H NMR, and ^{13}C NMR spectroscopic techniques were used to identify structures of the intermediate compounds (**1**, **2**, and **3**) and the target diamine monomer (**4**). Figure S1 in Supporting Information illustrates FTIR spectra of all the synthesized compounds. The nitro groups of compounds **1** and **3** gave two characteristic bands at around 1585 and 1321 cm^{-1} (—NO_2 asymmetric and symmetric stretching). After reduction, the characteristic absorptions of the nitro group disappeared and the amino group showed the typical N—H stretching absorption pair in the region of 3300–3500 cm^{-1}. The ^{1}H NMR and ^{13}C NMR spectra included in Supporting Information Figures S2–S4 confirm the structures of precursor compounds **1**∼**3**. Figure 1 illustrates the ^{1}H NMR and ^{13}C NMR spectra of the diamine monomer **4**. Assignments of each carbon and proton are assisted by the two-dimensional (2D) COSY NMR spectra shown in Supporting Information Figure S5, and the spectra agree well with the proposed molecular structure of **4**. The ^{1}H NMR spectra confirm that the nitro groups have been completely transformed into amino groups by the high field shift of the aromatic protons, especially for protons-f *ortho* to the amino group, and the resonance signal at around 5.0 ppm corresponding to the aryl primary amino protons. In addition, the elemental analysis result of **4** was in good agreement with the calculated values.

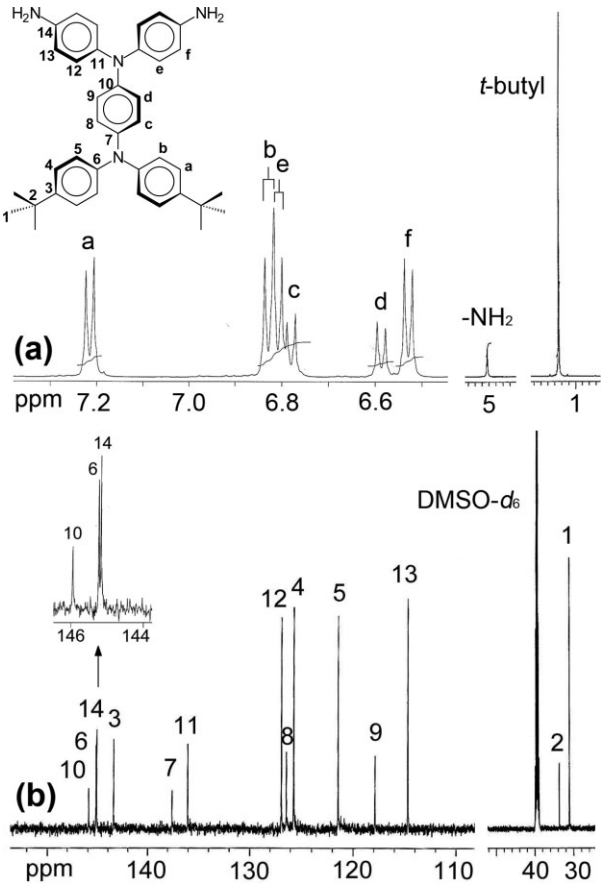

Figure 1. (a) ^{1}H NMR and (b) ^{13}C NMR spectra of the diamine monomer **4** in DMSO-d_6.

Polymer Synthesis

According to the phosphorylation polyamidation technique described by Yamazaki et al.,[31,32] a series of novel polyamides (**6a**–**6j**) with di-*tert*-butyl-substituted TPPA units were synthesized from the diamine **4** and various dicarboxylic acids **5a–5j** via solution polycondensation using TPP and pyridine as condensing agents (Scheme 2). All the polymerization proceeded homogeneously throughout the reaction and afforded clear and highly viscous polymer solutions, which precipitated in a tough, fiber-like form when the resulting polymer solutions were slowly poured into stirring methanol. As shown in Table 1, the obtained polyamides had inherent viscosities in the range of 0.29–0.71 dL/g and could be solution-cast into flexible and tough films, indicating high molecular weight polymers. The formation of polyamides was also confirmed by IR spectroscopy. A typical IR spectrum for polyamide **6a** is given in Supporting Information Figure S6. The characteristic IR absorption bands for the amide group appeared around 3300 (N—H stretching) and 1650 cm^{-1} (amide carbonyl).

Properties of the Polyamides

Solubility and Film Morphology

The solubility behavior of polyamides was tested qualitatively, and the results are also included in Table 1. All the polyamides were highly soluble in polar solvents such as NMP, DMAc, DMF, and *m*-cresol, and the high solubility could be attributed to the introduction of the three-dimensional TPPA moiety and bulky pendent *tert*-butyl substituents into the repeat unit. Thus, the excellent solubility makes these polymers potential

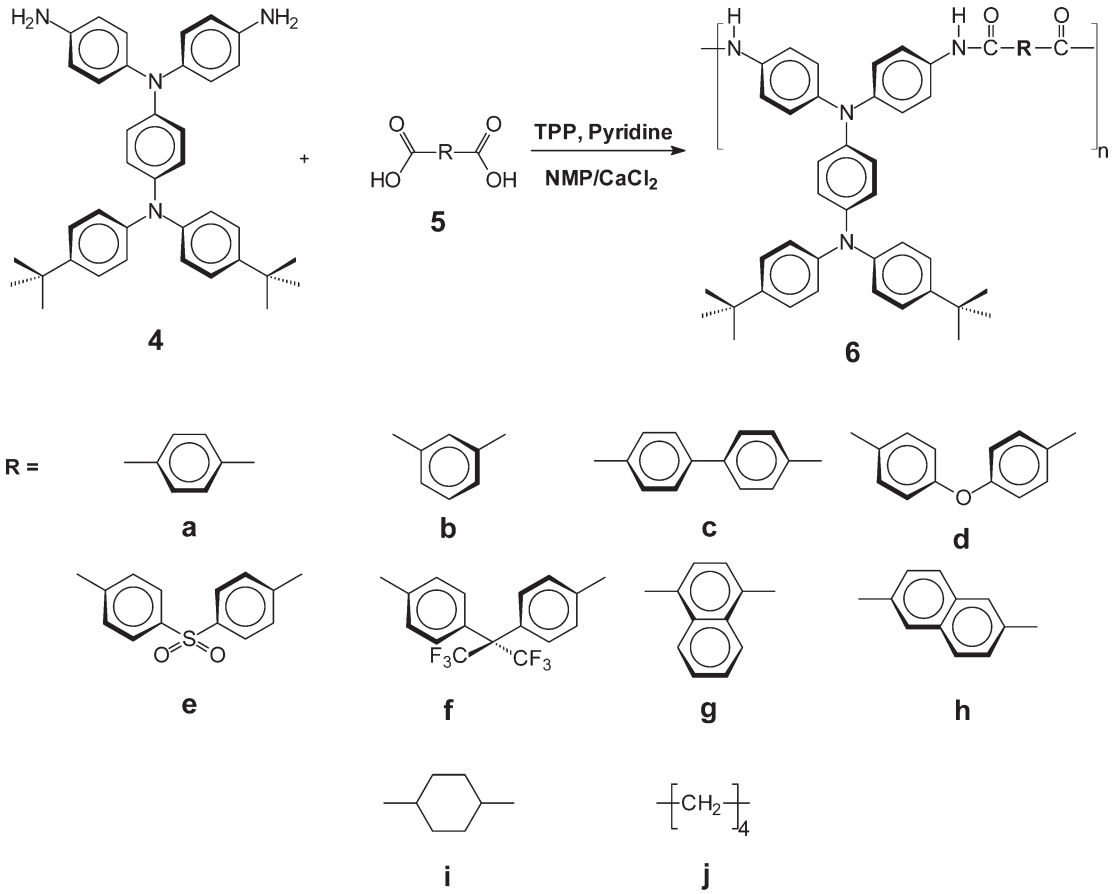

Scheme 2. Synthesis of polyamides **6a–6j**.

candidates for practical applications by spin-coating or inkjet-printing processes to afford high performance thin films for optoelectronic devices. The WAXD patterns of the polyamide films are shown in Supporting Information Figure S7. These polymers exhibited an amorphous nature because of the bulky, packing-disruptive di-*tert*-butyl-substituted TPPA unit which does not favor close chain packing. The amorphous nature of these polyamides was reflected not only in their good solubility but also in the UV–Vis absorption data of the polymers. The UV–Vis absorption peaks of the polymers do not shift from the solutions to the films, implying that there is no significant π-π interaction aggregation between the polymer chains.

Thermal Properties

The thermal properties of the polyamides were investigated by TGA, DSC, and TMA techniques. The thermal behavior data are summarized in Table 2. Typical TGA curves of the representative polyamide **6f** in both air and nitrogen atmospheres are depicted in Figure 2. All the aromatic polyamides exhibited good thermal stability with no remarked weight loss up to 450 °C in nitrogen or in air. Their decomposition temperatures (T_d) at a 10% weight-loss in nitrogen and air were recorded at 544–569 °C and 517–560 °C, respectively. The carbonized residue (char yield) of these aromatic polymers was >62% at 800 °C in nitrogen atmosphere. The high char yields of these polymers could be ascribed to their high aromatic content. The glass-transition temperatures (T_g) of all the aromatic polyamides were observed in the range of 269–296 °C by DSC and decreased with rigidity and symmetry of the dicarboxylic acid components. The T_s values of the polymer films were determined from the onset temperature of the probe displacement on the TMA trace. A typical TMA thermogram for polyamide **6f** is also illustrated in Figure 2. In most cases, the T_s values obtained by TMA were slightly lower than the T_g values measured by the DSC experiments. These differences may also be attributed to the

Table 1. Inherent Viscosity and Solubility of Polyamides

Polymer Code	η_{inh}[a] (dL/g)	Solubility in Various Solvents[b]					
		NMP	DMAc	DMF	DMSO	*m*-Cresol	THF
6a	0.71	+ +	+ +	+ +	±	+ +	±
6b	0.35	+ +	+ +	+ +	±	+ +	+ +
6c	0.71	+ +	+ +	+ +	±	+ +	±
6d	0.63	+ +	+ +	+ +	±	+ +	±
6e	0.48	+ +	+ +	+ +	±	+ +	+ +
6f	0.51	+ +	+ +	+ +	±	+ +	+ +
6g	0.29	+ +	+ +	+ +	±	+ +	±
6h	0.56	+ +	+ +	+ +	±	+ +	±
6i	0.60	+ +	+ +	+ +	±	+ +	±
6j	0.45	+ +	+ +	+ +	±	+ +	±

[a] Measured at a polymer concentration of 0.5 g/dL in DMAc-5 wt % LiCl at 30 °C.
[b] The qualitative solubility was tested with 10 mg of a sample in 1 mL of stirred solvent. Notation: + +, soluble at room temperature; ±, partially soluble; NMP, *N*-methyl-2-pyrrolidone; DMAc, *N*,*N*-dimethylacetamide; DMF, *N*,*N*-dimethylformamide; DMSO, dimethyl sulfoxide; THF, tetrahydrofuran.

different heating story of the samples and the distinct nature of these two testing methods. As expected, the semiaromatic polyamides **6i** and **6j** revealed a lower T_g, T_s, T_d, and char yield when compared with those of the aromatic ones because of the more flexible and less stable aliphatic segments. There is a large window between T_g or T_s and the decomposition temperature of each polymer especially for **6j**, which could be advantageous in the processing of these polymers by the thermoforming technique.

Optical and Electrochemical Properties

The optical properties of the polyamides were investigated by UV–Vis and PL spectroscopy. The

Table 2. Thermal Properties of Polyamides[a]

Polymer Code	T_g (°C)[b]	T_s (°C)[c]	T_d at 5% Weight Loss (°C)[d]		T_d at 10% Weight Loss (°C)[d]		Char Yield (wt %)[e]
			In N_2	In Air	In N_2	In Air	
6a	287	273	508	471	569	524	71
6b	279	273	531	461	569	518	66
6c	296	283	485	460	545	517	71
6d	269	264	500	483	548	542	68
6e	296	280	511	475	544	517	62
6f	287	272	522	502	564	560	64
6g	282	260	517	495	552	553	65
6h	285	267	488	473	548	533	72
6i	253	250	440	421	462	471	30
6j	207	198	404	405	425	445	25

[a] The polymer film samples were heated at 300 °C for 30 min before all the thermal analyses.
[b] Midpoint temperature of the baseline shift on the second DSC heating trace (rate = 20 °C/min) of the sample after quenching from 400 to 50 °C (rate = −200 °C/min) in nitrogen.
[c] Softening temperature measured by TMA with a constant applied load of 10 mN at a heating rate of 10 °C/min.
[d] Decomposition temperature at which a 5 or 10% weight loss was recorded by TGA at a heating rate of 20 °C/min and a gas flow rate of 40 cm^3/min.
[e] Residual weight percentage at 800 °C in nitrogen.

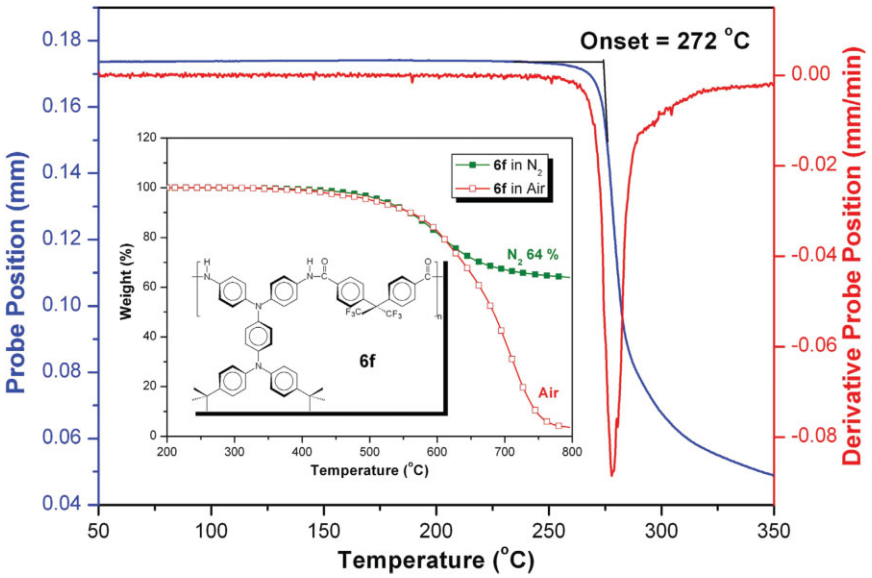

Figure 2. TMA and TGA curves of polyamide **6f** with a heating rate of 10 °C/min and 20 °C/min, respectively. [Color figure can be viewed in the online issue, which is available at www.interscience.wiley.com.]

results are summarized in Table 3. These polymers exhibited strong absorption bands at λ_{max} = 309–355 nm in NMP solutions, which are mainly assignable to the combinations of π-π* and n-π* transitions resulting from the conjugated TPPA units. In the solid state, the polyamides showed absorption characteristics (λ_{max} around 316–342 nm) similar to those observed in solutions. Their PL spectra in dilute NMP solution showed emission maxima around 360–448 nm in the violet-

Table 3. Optical and Electrochemical Properties of the Polyamides

	In Solution			As Film		Oxidation Potential (V)[c]				HOMO (eV)[e]		LUMO (eV)[f]	
						First		Second					
Polymer	Abs λ_{max} (nm)[a]	PL λ_{max} (nm)[a]	Φ_{PL} (%)[b]	Abs λ_{max} (nm)	Abs λ_{onset} (nm)	$E_{1/2}$	E_{onset}	$E_{1/2}$	E_g (eV)[d]	$E_{1/2}$	E_{onset}	$E_{1/2}$	E_{onset}
6a	309	362	2.69	311	448	0.58	0.44	0.96	2.77	4.94	4.80	2.17	2.63
6b	350	434	1.27	316	419	0.59	0.46	0.97	2.96	4.95	4.82	1.99	1.86
6c	305	360	1.39	310	456	0.59	0.42	0.97	2.72	4.95	4.78	2.23	2.06
6d	349	439	0.86	338	412	0.59	0.47	0.96	3.01	4.95	4.83	1.94	1.82
6e	325	390	1.29	311	428	0.59	0.45	0.97	2.90	4.95	4.81	2.05	1.91
6f	355	448	0.77	310	429	0.57	0.47	0.95	2.76	4.93	4.83	2.17	2.07
6g	327	398	0.73	316	412	0.60	0.49	0.95	2.89	4.96	4.85	2.07	1.96
6h	312	367	1.27	309	479	0.58	0.47	0.98	2.59	4.94	4.83	2.35	2.24
6i	330	415	13.10	332	397	0.57	0.46	0.94	3.12	4.93	4.82	1.81	1.70
6j	329	415	15.10	335	391	0.58	0.42	0.93	3.17	4.94	4.78	1.77	1.61
6′d	347	461	0.28	347	415	0.57	0.44	0.95	2.99	4.93	4.80	1.94	1.81

[a] Measured at a concentration of $\sim 10^{-5}$ mol/L in NMP.
[b] The quantum yield in dilute solution was calculated in an integrating sphere with quinine sulfate as the standard (Φ_{PL} = 54.6 %).
[c] From cyclic votammograms versus Ag/AgCl in CH_3CN. $E_{1/2}$: half-wave potential.
[d] Energy gap = 1240/Abs λ_{onset} of the polymer film.
[e] The HOMO energy levels were calculated from $E_{1/2}$ or E_{onset} and were referenced to ferrocene (4.8 eV).
[f] LUMO = HOMO − E_g.

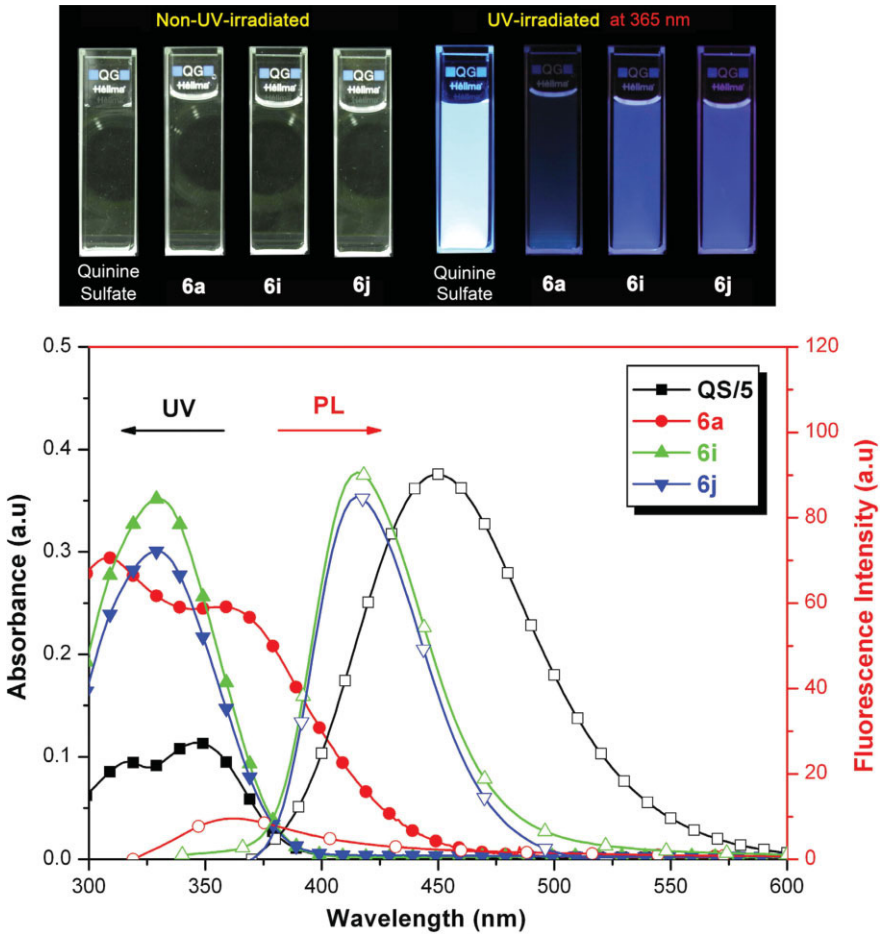

Figure 3. UV–Vis absorption and PL spectra of the dilute solutions of polyamides **6a**, **6i**, and **6j** in NMP (1×10^{-5} M). Quinine sulfate dissolved in 1 M H_2SO_4 (aq.) with a concentration of 1×10^{-5} M as the standard ($\Phi_{PL} = 54.6\%$). Photographs show the appearance of the sample solutions before and after exposure to a standard laboratory UV lamp.

to-blue region. Figure 3 shows the typical UV–Vis absorption and PL spectra of the representative polyamides **6a**, **6i**, and **6j** in NMP (concentration: 1×10^{-5} mol/L). These polyamides in NMP solution exhibited fluorescence emission maxima at 360–448 nm with quantum yields ranging from 0.73% for **6g** to 15.10% for **6j**. The aromatic–aliphatic polyamides **6i** and **6j** exhibited higher fluorescence quantum yields compared with the aromatic polyamides **6a**–**6h**. This could be attributed to the less charge transfer complexing between the aliphatic segment in the diacid component and the TPPA unit in the diamine component.

The electrochemical behavior of the **6** series polyamides was investigated by CV conducted for the cast film on the ITO-coated glass substrate as the working electrode in dry acetonitrile (CH_3CN) containing 0.1 M of TBAP as an electrolyte under nitrogen atmosphere. The typical cyclic voltammograms for polyamide **6d** (with the *tert*-butyl substituents on the TPPA unit) and **6′d** (without the *tert*-butyl substituents) are shown in Figure 4 for comparison. There are two reversible oxidation redox couples at half-wave potentials ($E_{1/2}$) of 0.59 and 0.96 V, respectively, for polyamide **6d** in the oxidative scan. The color of the film changed from colorless to green and then to deep blue upon electrochemical oxidation of the TPPA unit in the polymer chain. Polyamide **6d** still exhibited excellent redox and electrochromic reversibility even after over 500 continuous cyclic scans between 0.0 and 1.2 V. On the contrary, the corresponding polyamide **6′d** without the *tert*-butyl substituents on its TPPA unit gradually lost redox reversibility after 100 times cycling. The introduction of bulky

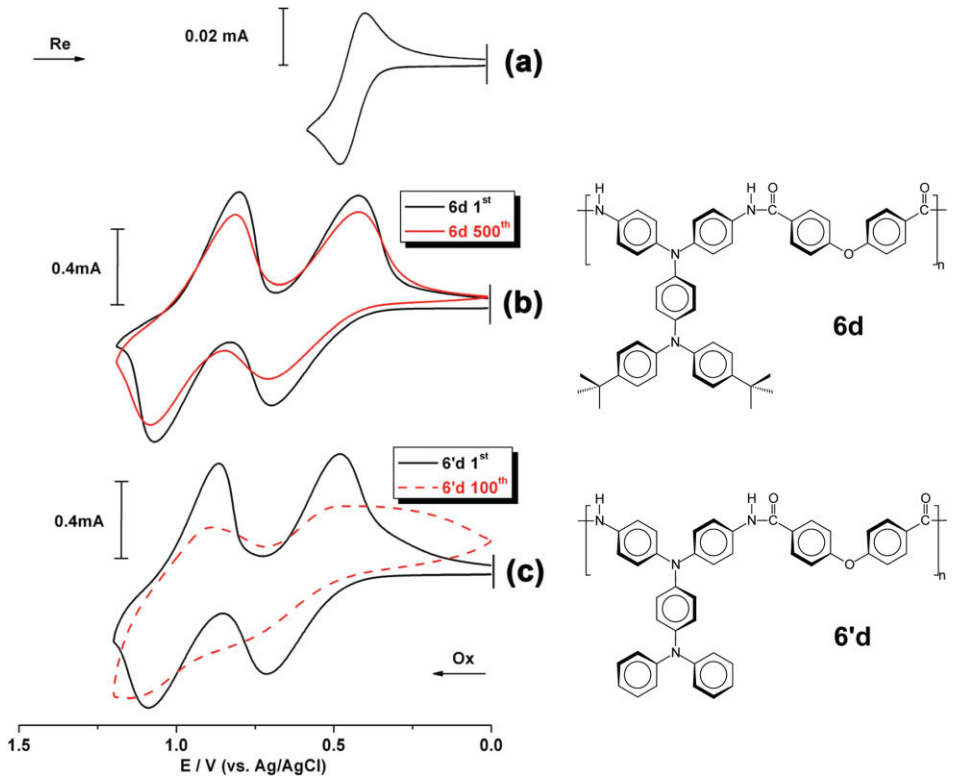

Figure 4. Cyclic voltammograms of (a) ferrocene and the cast films of (b) polyamide **6d** and (c) polyamide **6′d** on an ITO-coated glass slide in CH_3CN containing 0.1 M TBAP at a scanning rate of 0.1 V/s. [Color figure can be viewed in the online issue, which is available at www.interscience.wiley.com.]

tert-butyl group greatly prevents the coupling reaction of the electroactive polyamides **6** when compared with the corresponding polyamides **6′** without *tert*-butyl substituent (see Supporting Information Figure S8). Thus, the incorporation of bulky *tert*-butyl groups on the active sites of the TPPA unit lends considerable stability to both the cation radical and dication of the TPPA moiety. The redox potentials of the various polyamides as well as their highest occupied molecular orbital (HOMO) and lowest unoccupied molecular orbital (LUMO) levels (below vacuum) are also listed in Table 3. The external ferrocene/ferrocenium (Fc/Fc+) redox standard has $E_{1/2}$ and E_{onset} of 0.44 and 0.37 V versus Ag/AgCl in acetonitrile. The $E_{1/2}$ of Fc/Fc+ is known to be 4.80 eV below the vacuum level and was used as a calibration reference. Thus, the HOMO levels for polyamides **6a–6j** were evaluated to be 4.78–4.85 eV and 4.93–4.96 eV calculated from E_{onset} and $E_{1/2}$, respectively. The lower ionization potential could suggest an easier hole-injection into films from ITO electrodes in electronic device applications. Traditionally, introduction of triarylamine units

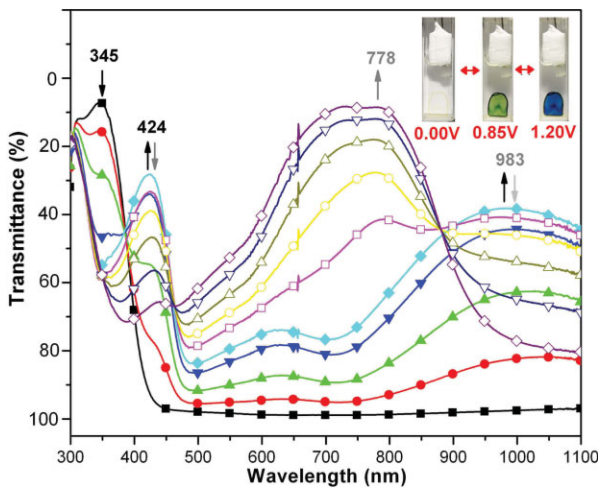

Figure 5. Spectral change of polyamide **6d** thin film on the ITO-coated glass slide (in CH_3CN with 0.1 M TBAP as the supporting electrolyte) along with increasing of the applied voltage: 0.0 (■), 0.55 (●), 0.65 (▲), 0.75 (▼), 0.85 (◆), 0.95 (□), 1.00 (○), 1.05 (Δ), 1.10 (▽), and 1.20 V (◇) (vs. Ag/AgCl). The inset shows the photographic images of the film at indicated electrode potentials. [Color figure can be viewed in the online issue, which is available at www.interscience.wiley.com.]

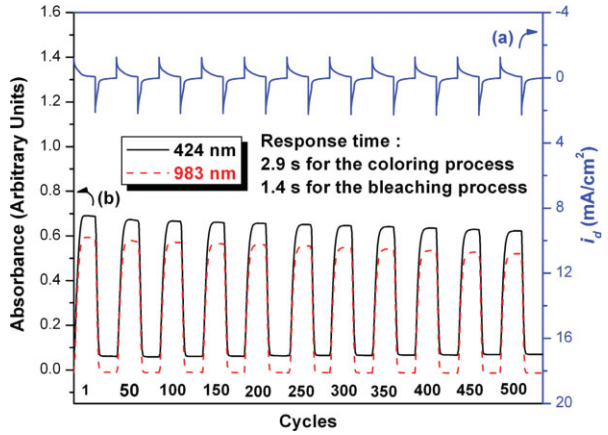

Figure 6. (a) Current consumption and (b) electrochromic switching between 0 and 0.85 V and optical absorbance change monitored at 424 and 983 nm for polyamide **6d** in 0.1 M TBAP/CH_3CN with a cycle time of 20 s. [Color figure can be viewed in the online issue, which is available at www.interscience.wiley.com.]

in conjugated polymers or organic molecules was found to effectively enhance the hole-injecting properties of the resulting materials.[33–37]

Spectroelectrochemical and Electrochromic Properties

Spectroelectrochemical experiments were conducted to elucidate the optical characteristics of the electrochromic films. For these investigations, the polyamide film was cast on an ITO-coated glass slide (a piece that fit in the commercial UV–Vis cuvette), and a homemade electrochemical cell was built from a commercial UV–Vis cuvette. The cell was placed in the optical path of the sample light beam in a commercial diode array spectrophotometer. This procedure allowed us to obtain electronic absorption spectra under potential control in a 0.1 M TBAP/acetonitrile solution. The result of the polyamide **6d** film is presented in Figure 5 as a series of UV–Vis absorbance curves correlated to electrode potentials. In its neutral state, the film exhibited strong absorption at wavelength around 345 nm, characteristic for triarylamine, but it was almost transparent in the visible region. When the applied voltage was stepped from 0 to 0.85 V, the intensity of the absorption peak at 345 nm gradually decreased while a new peak at 424 nm and a broad band having its maximum absorption wavelength at 983 nm in the near-infrared (NIR) region gradually increased in intensity. We attribute this spectral change to the formation of a stable monocation radical of the TPPA moiety. When the potential was adjusted to a more positive value of 1.2 V, the absorption bands of the cation radical decreased gradually in intensity, with a formation of a new strong absorption band centered at about 778 nm. This spectral change can be attributable to the formation of a dication in the TPPA unit of the polyamide. The observed UV–Vis absorption changes in the film of **6d** at various potentials are fully reversible and are associated with drastic color changes. From the inset shown in Figure 5, it can be seen that the film of polyamide **6d** switches from a transmissive neutral state (nearly colorless) to a highly absorbing semioxidized state (green) and a fully oxidized state (blue). Polymer **6d** exhibited high optical contrast in the visible and NIR regions, with a high percent transmittance change (ΔT %) of 64% at 424 nm and 59% at 983 nm for green coloring and 90% at 778 nm for blue coloring.

For electrochromic switching studies, polymer films were cast on ITO-coated glass slides in the same manner as described earlier, and each film was potential stepped between its neutral (0 V) and oxidized (+0.85 V) state. While the films were switched, the absorbance at 983 nm was monitored as a function of time with UV–Vis-NIR spectroscopy. Switching data for the cast films of polyamides **6d** and **6′d** are given in Figures 6 and 7, respectively. The switching time was calculated at 90% of the full switch because it is difficult to perceive any further color change with naked eye beyond this point. As depicted in Supporting

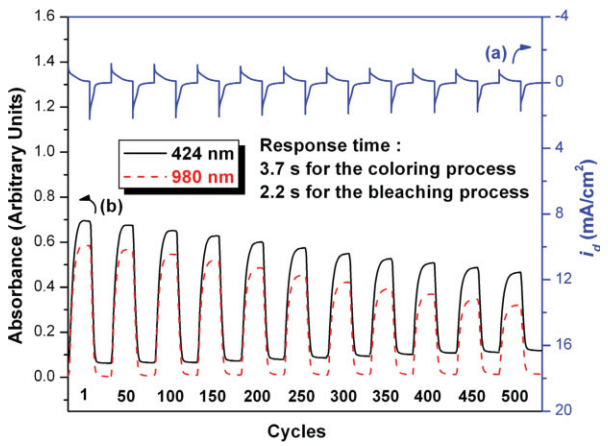

Figure 7. (a) Current consumption and (b) electrochromic switching between 0 and 0.85 V and optical absorbance change monitored at 424 and 983 nm for polyamide **6′d** in 0.1 M TBAP/CH_3CN with a cycle time of 20 s. [Color figure can be viewed in the online issue, which is available at www.interscience.wiley.com.]

Table 4. Optical and Electrochemical Data Collected for Coloration Efficiency Measurements of Polyamides **6d** and **6′d**

Cycling Times[a]	ΔOD[b]		Q (mC/cm^2)[c]		η (cm^2/C)[d]		Decay (%)[e]	
	6d	**6′d**	**6d**	**6′d**	**6d**	**6′d**	**6d**	**6′d**
1	0.581	0.584	2.69	2.88	216	203	0	0
50	0.575	0.565	2.71	3.04	212	186	1.85	8.37
100	0.570	0.545	2.69	3.02	212	181	1.85	10.84
150	0.565	0.517	2.66	2.94	212	176	1.85	13.30
200	0.560	0.486	2.67	2.82	210	172	2.78	15.27
250	0.555	0.454	2.66	2.71	209	167	3.24	17.73
300	0.547	0.422	2.65	2.57	206	164	4.63	19.21
350	0.542	0.394	2.64	2.44	205	161	5.37	20.69
400	0.535	0.368	2.63	2.37	203	155	6.31	23.65
450	0.527	0.347	2.62	2.26	201	153	6.94	24.63
500	0.519	0.322	2.59	2.13	200	151	7.41	25.62

[a] Switching between 0 and 0.85 V (vs. Ag/AgCl).
[b] Optical density change at 983 nm for **6d** and 980 nm for **6′d**.
[c] Ejected charge, determined from the *in situ* experiments.
[d] Coloration efficiency is derived from the equation: $\eta = \Delta OD/Q$.
[e] Decay of coloration efficiency after various cyclic scans.

Information Figure S9, thin film from polyamide **6d** revealed switching time of 2.9 s for $\lambda_{max} = 983$ nm and 2.4 s for bleaching, reflecting the different reaction rates between the neutral and oxidized forms of the film of **6d**. The polyamides switch rapidly (within 3 s) between the highly transmissive neutral state and the colored oxidized state. CE (η) was measured by monitoring the amount of ejected charge (Q) as a function of the change in optical density (ΔOD) of the polymer film.[38,39] The electrochromic CEs ($\eta = \Delta OD/Q$) of the polymer films of **6d** and **6′d** after various switching cycles are summarized in Table 4. After switching 500 times between 0 and 0.85 V, the film of polyamide **6d** only showed 7.41% decay on CE, which is much lower than that of corresponding **6′d** analogue. Therefore, the results of these experiments revealed that the introduction of the *tert*-butyl group at the active sites of the TPPA unit enhances the redox and electrochromic stability of these polymers.

CONCLUSIONS

A new TPPA-based aromatic diamine monomer, *N*,*N*-bis(4-aminophenyl)-*N*′,*N*′-bis(4-*tert*-butylphenyl)-1,4-phenylenediamine, was synthesized in high purity and high yields from readily available reagents. A series of novel polyamides with di-*tert*-butyl-substituted TPPA moieties were readily prepared from the newly synthesized diamine monomer with various aromatic or aliphatic dicarboxylic acids via the phosphorylation polyamidation reaction. Introduction of bulky *tert*-butyl substituents at the active sites of TPPA segment not only stabilizes arylaminium cationic radicals and dications but also leads to good solubility and film-forming properties of the polyamides. In addition to high T_g or T_s values and good thermal stability, all the obtained polymers also reveal valuable electrochromic characteristics such as high contrast ratio and high CE. The color changes from the colorless or pale yellowish neutral form to the green and blue oxidized forms when scanning potentials positively from 0.0 to 1.2 V. After >500 cyclic switches, the polymer films still exhibited excellent redox and electrochromic reversibility. Thus, these characteristics suggest that the present polyamides have great potential for use in opto-electronic applications.

This work was supported by National Science Council of Taiwan, Republic of China (Grant no. NSC 97-2221-E-027-113-MY3).

REFERENCES AND NOTES

1. Monk, P. M. S.; Mortimer, R. J.; Rosseinsky, D. R. Electrochromism: Fundamentals and Applications; VCH: Weinheim, Germany, 1995.

2. Monk, P. M. S.; Mortimer, R. J.; Rosseinsky, D. R. Electrochromism and Electrochromic Devices; Cambridge University Press: Cambridge, UK, 2007.
3. Rosseinsky, D. R.; Mortimer, R. J. Adv Mater 2001, 13, 783–793.
4. Walczak, R. M.; Reynolds, J. R. Adv Mater 2006, 18, 1121–1131.
5. Argun, A. A.; Aubert, P. H.; Thompson, B. C.; Schwendeman, I.; Gaupp, C. L.; Hwang, J.; Pinto, N. J.; Tanner, D. B.; MacDiarmid, A. G.; Reynolds, J. R. Chem Mater 2004, 16, 4401–4412.
6. Groenendaal, L.; Zotti, G.; Aubert, P.-H.; Waybright, S. M.; Reynolds, J. R. Adv Mater 2003, 15, 855–879.
7. Groenendaal, L.; Jonas, F.; Freitag, D.; Pielartzik, H.; Reynolds, J. R. Adv Mater 2000, 12, 481–494.
8. Roncali, J.; Blanchard, P.; Frere, P. J Mater Chem 2005, 15, 1589–1610.
9. Durmus, A.; Gunbas, G. E.; Toppare, L. Chem Mater 2007, 19, 6247–6251.
10. Thelakkat, M. Macromol Mater Eng 2002, 287, 442–461.
11. Shirota, Y. J Mater Chem 2005, 15, 75–93.
12. Leung, M.-K.; Chou, M.-Y.; Su, Y.-L.; Chiang, C.-L.; Chen, H.-L.; Yang, C.-F.; Yang, C.-C.; Lin, C.-C.; Chen, H.-T. Org Lett 2003, 5, 839–842.
13. Chou, M.-Y.; Leung, M.;-K.; Su, Y.-L.; Chiang, C.-L.; Lin, C.-C.; Liu, J.-H.; Kuo, C.-K.; Mou, C.-Y. Chem Mater 2004, 16, 654–661.
14. Beaupre, S.; Dumas, J.; Leclerc, M. Chem Mater 2006, 18, 4011–4018.
15. Natera, J.; Otero, L.; Sereno, L.; Fungo, F.; Wang, N.-S.; Tsai, Y.-M.; Hwu, T.-Y.; Wong, K.–T. Macromolecules 2007, 40, 4456–4463.
16. Cheng, S.-H.; Hsiao, S.-H.; Su, T.-H.; Liou, G.–S. Macromolecules 2005, 38, 307–316.
17. Su, T.-H.; Hsiao, S.-H.; Liou, G.-S. J Polym Sci Part A: Polym Chem 2005, 43, 2085–2098.
18. Liou, G.-S.; Hsiao, S.-H.; Su, T.-H. J Mater Chem 2005, 15, 1812–1820.
19. Liou, G.-S.; Hsiao, S.-H.; Chen, H.-W. J Mater Chem 2006, 16, 1831–1842.
20. Liou, G.-S.; Hsiao, S.-H.; Huang, N.-K.; Yang, Y.-L. Macromolecules 2006, 39, 5337–5346.
21. Liou, G.-S.; Hsiao, S.-H.; Chen, W.-C.; Yen, H.-J. Macromolecules 2006, 39, 6036–6045.
22. Hsiao, S.-H.; Liou, G.-S.; Kung, Y.-C.; Yen, H.-J. Macromolecules 2008, 41, 2800–2808.
23. Seo, E. T.; Nelson, R. F.; Fritsch, J. M.; Marcoux, L. S.; Leedy, D. W.; Adams, R. N. J Am Chem Soc 1966, 88, 3498–3503.
24. Zhao, H.; Tanjutco, C.; Thayumanavan, S. Tetrahedron Lett 2001, 42, 4421–4424.
25. Hsiao, S.-H.; Chang, Y.-M.; Chen, H.-W.; Liou, G.-S. J Polym Sci Part A: Polym Chem 2006, 44, 4579–4592.
26. Chang, C.-W.; Liou, G.-S.; Hsiao, S.-H. J Mater Chem 2007, 17, 1007–1015.
27. Liou, G.-S.; Chang, C.-W. Macromolecules 2008, 41, 1667–1674.
28. Chang, C.-W.; Chung, C.-H.; Liou, G.-S. Macromolecules 2008, 41, 8441–8451.
29. Chang, C.-W.; Liou, G.-S. J Mater Chem 2008, 18, 5638–5646.
30. Demas, J. N.; Crosby, G. A. J Phys Chem 1971, 75, 991–1024.
31. Yamazaki, N.; Higashi, F.; Kawabata, J. J Polym Sci: Polym Chem Ed 1974, 12, 2149–2154.
32. Yamazaki, N.; Matsumoto, M.; Higashi, F. J Polym Sci: Polym Chem Ed 1975, 13, 1375–1380.
33. Pu, Y.-J.; Soma, M.; Kido, J.; Nishide, H. Chem Mater 2001, 13, 3817–3819.
34. Liang F.-S.; Pu, Y.-J.; Kurata, T.; Kido J.; Nishide, H. Polymer 2005, 46, 3767–3781.
35. Liang F.-S.; Kurata, T.; Nishide, H.; Kido, J. J Polym Sci Part A: Polym Chem 2005, 43, 5765–5773.
36. Kim, Y.-H.; Zhao, Q.-H.; Kwon, S.-K. J Polym Sci Part A: Polym Chem 2006, 44, 172–182.
37. Zhao, Q.-H.; Kim, Y.-H.; Dang T. T. M.; Shin, D.-C.; You, H.; Kwon, S.-K. J Polym Sci Part A: Polym Chem 2007, 45, 341–347.
38. Gaupp, C. L.; Welsh, D. M.; Rauh, R. D.; Reynolds, J. R. Chem Mater 2002, 14, 3964–3970.
39. Mortimer, R. J.; Reynolds, J. R. J Mater Chem 2005, 15, 2226–2233.